Phytopathology Research

RESEARCH

Open Access

Editing of the rice importin gene *IMPα1b* results in sequestration of TAL effectors from plant cell nuclei

Jinfeng Peng[1], Jingyuan Nie[1], Xiaochen Chen[2,3], Liyuan Zhang[2,3], Xiaohui Yao[2,3], Ping Li[4], Huicong Shi[4], Congfeng Song[1*] and Hansong Dong[1,2,3*]

Abstract

Transcription activator-like effectors (TALEs) produced by plant pathogenic bacteria mainly belonging to the genus *Xanthomonas* cause plant diseases through activation of host susceptibility genes in plant cell nuclei. How TALEs enter plant cell nuclei was not clear until recent studies about PthXo1 and TALI, two TALEs produced by *Xanthomonas oryzae* pv. *oryzae* (*Xoo*) and *X. oryzae* pv. *oryzicola* (*Xoc*), the rice (*Oryza sativa*) pathogens that cause bacterial blight and bacterial leaf streak, respectively. Here, we report that rice importin IMPα1b serves as a nuclear transport receptor in rice plants to facilitate the nuclear import of PthXo1 and TALI from *Xoo* and *Xoc*, respectively. While wild-type (WT) rice plants support the nuclear import of PthXo1 and TALI, nuclear trafficking is defective in *OsIMPα1b* loss-of-function mutants generated by clustered regularly interspaced short palindromic repeats (CRISPR)–CRISPR-associated 9 (Cas9)-based gene editing. In the edited plants infected by *Xoo*, OsIMPα1b sequesters PthXo1 from the nucleus, the PthXo1-targeted rice susceptibility gene is no longer activated, and bacterial virulence and blight disease are alleviated as a result. In the edited plants infected by *Xoc*, OsIMPα1b sequesters TALI from the nucleus, the role of TALI in suppressing rice defense responses is nullified, and rice defense responses are in turn activated to inhibit bacterial virulence and alleviate bacterial leaf streak severity.

Keywords: Importin, *IMPα1*, Bacterial blight, Transcription activator-like effector (TALE), PthXo1, TALI, Translocation, Nuclear import

Background

Plant-pathogenic gram-negative bacteria use the type III (T3) secretion system to secrete a large number of pathogenicity determinants called T3 effectors (Büttner 2012; Bundalovic-Torma et al. 2022). T3 effectors can play a role in the virulence of bacteria, resulting in diseases in susceptible varieties of host plants (Chen et al. 2021), and they can be an avirulent factor, inducing defense responses in nonhost plants or resistant varieties of host plants (Wang et al. 2018). To exert these distinct functions, T3 effectors must be translocated from bacteria into plant cells (Büttner 2012; Li et al. 2019; Chen et al. 2021; Hajra et al. 2021; Bergeron and Marlovits 2022). Depending on their locations in plant cells, T3 effectors are translocated via a shorter trafficking route toward the cell cytosol or a longer route toward the cell nucleus.

The longer and shorter trafficking routes apply to bacterial transcription activator-like effectors (TALEs) and non-TAL effectors (nTALEs), respectively (Deng et al. 2012; Hui et al. 2019). nTALE translocation may occur via a T3 translocon (Picking and Barta 2019), which is thought to be formed by molecular interactions of bacterial proteinic translocators with each other and with

*Correspondence: cfsong@njau.edu.cn; hsdong@sdau.edu.cn

[1] College of Plant Protection, Nanjing Agricultural University, Nanjing 210095, China
Full list of author information is available at the end of the article

their receptors situated in plasma membranes (PMs) of plant cells (Büttner 2012; Ji and Dong 2015; Zhang et al. 2019a). Due to variations in the translocator repertoire present in different bacteria, endocytosis of effectors may occur by direct interactions with recognition compounds in plant PMs (Santi-Rocca and Blanchard 2017; Gaytán et al. 2018; Wagner et al. 2018; Shanmugam and Dalbey 2019). Thus, a translocon-dependent route or a translocon-independent route may be used to transport nTALEs into the cytosol of plant cells (Zhang et al. 2019a). In contrast, TALEs need to be first translocated into the cytosol by a translocon or via endocytosis and then delivered into the nucleus (Bogdanove and Voytas 2011; Wang et al. 2017; Hui et al. 2019) by molecular trafficking with the aid of plant importins (Wirthmueller et al. 2013; Roth et al. 2017; Zhao et al. 2019; Xiong et al. 2021). Characterizing plant importins that transport bacterial TALEs into plant cell nuclei has been an important subject in phytopathology research (Wirthmueller et al. 2015; Jo et al. 2017; Roth et al. 2017; Schäfer et al. 2017; Hui et al. 2019).

The gram-negative bacteria *Xanthomonas oryzae* pv. *oryzae* (*Xoo*) and *X. oryzae* pv. *oryzicola* (*Xoc*) are devastating bacterial pathogens of rice (*Oryza sativa*), causing bacterial blight (BB) and bacterial leaf streak (BLS), respectively, via virulence functions of either nTALEs known as *Xanthomonas* outer proteins (Xops) or TALEs (White et al. 2009). Both Xops and TALEs are translocated via bacterial T3 translocators and their receptors in plant PMs (Büttner et al. 2002; Büttner and Bonas 2002; Li et al. 2011; Ji and Dong 2015; Bian et al. 2019; Li et al. 2019; Mo et al. 2020; Chen et al. 2021). T3 translocators already identified in *Xoo* and *Xoc* include Hpa1, HrpF, and XopN (Li et al. 2011; Wang et al. 2018; Mo et al. 2020; Chen et al. 2021). XopN interacts with a receptor-like protein kinase located in plant PMs (Kim et al. 2009) and facilitates *Xoo* effector translocation into rice cells (Mo et al. 2020). Bacterial HrpF facilitates T3 effector translocation, possibly by interacting with PM lipids (Büttner et al. 2002; Li et al. 2011). In rice, OsPIP1;3, an aquaporin of the PM intrinsic protein (PIP) family, has been identified as the receptor for bacterial Hpa1 (Li et al. 2019; Chen et al. 2021).

In *Xoo*-infected rice plants, Hpa1 is secreted via the bacterial T3 secretion system and serves as a translocator of the TALE PthXo1 secreted through the same pathway (Wang et al. 2018). PthXo1 determines the virulence of the standard *Xoo* strain PXO99^{A} on the susceptible rice variety Nipponbare (Yang et al. 2006). To infect Nipponbare plants, PXO99^{A} secretes Hpa1 and delivers it to the plant–bacterium interface, where Hpa1 interacts with OsPIP1;3 to expedite translocation of the subsequently secreted PthXo1 (Bian et al. 2019; Li et al. 2019; Chen et al. 2021). Thereafter, PthXo1 induces virulence through activating the host susceptibility gene *OsSWEET11* (Yang et al. 2006) in an OsPIP1;3-dependent manner (Bian et al. 2019; Li et al. 2019). Similarly, Hpa1–OsPIP1;3 interactions are also critical for TALI translocation to induce BLS in Nipponbare plants (Chen et al. 2021). TALI is a TALE that was identified in the *Xoc* hypervirulent Chinese strain GD41 and determines virulence in the susceptible rice variety Nipponbare (Long et al. 2021). Extensive studies have shown that bacterial T3 translocators and their receptors on plant PMs function cooperatively to facilitate TALE translocation into the cytosol of plant cells (Büttner et al. 2002; Li et al. 2011; Bian et al. 2019; Li et al. 2019; Mo et al. 2020; Chen et al. 2021). However, these findings also raise questions about the next step of TALE trafficking in plant cells. How do bacterial TALEs move into plant cell nuclei? Do any plant importins play a role in nuclear trafficking? Do TALE-transporting importins affect plant growth and development?

Importins present in eukaryotic cells are cargo-transporting nucleocytoplasmic trafficking proteins that serve as nuclear transport receptors or as carriers for cytoplasmic proteins that have a nuclear localization signal (NLS). Typically, importins have a cargo-binding α-subunit (IMPα) that perceives NLS-containing cytosolic proteins and a cargo-navigating β-subunit (IMPβ) that facilitates transport of cytosolic proteins into plant nuclei (Merkle 2003). In general, IMPα recognizes a short positively charged NLS, while IMPβ mediates interactions with nuclear protein complexes and RanGTP to complete cargo transport (Xiong et al. 2021). In particular, RanGTP binds to IMPs (α and β) to induce cargo release into the nucleus and then brings IMPs back to the cytosol, where IMPs prepare for the next round of nuclear trafficking (Stewart 2007; Ems-McClung et al. 2020). IMPα has three key conserved structural features (Goldfarb et al. 2004): an N-terminal IMPβ-binding (IBB) domain, a series of armadillo (Arm) repeats, and a C-terminal acidic cluster (AC) motif. The Arm repeats serve as internal cargo NLS-binding sites, whereas the AC motif functions as a binding site for the nuclear export of IMPα in conjunction with RanGTP (Miyamoto et al. 2016). These features enable IMPα to effectively function in nucleocytoplasmic trafficking in a recycling manner (Lüdke et al. 2021).

In plants, both IMPα and IMPβ exist as multiple isoforms that are often associated with responses to pathogen attack (Lüdke et al. 2021; Xiong et al. 2021) and environmental stress (Merkle 2003). In rice, there are at least 16 importins, each designated as an OsIMP (Additional file 1: Table S1), although only OsIMPα1a and OsIMPα1b have been implicated in bacterial virulence in rice (Hui et al. 2019). OsIMPα1a and OsIMPα1b have

been shown to transport NLS-containing proteins (Jiang et al. 2001; Chang et al. 2012, 2014). Moreover, Hui et al. (2019) found that both OsIMPα1a and OsIMPα1b interact with PthXo1 in yeast, tobacco, and rice. They further demonstrated that, in a susceptible rice variety, silencing of *OsIMPα1a* or *OsIMPα1b* considerably enhances resistance to both *Xoo* and *Xoc*, along with marked alleviation of the disease severities of BB and BLS (Hui et al. 2019). Thus, OsIMPα1a and OsIMPα1b might facilitate bacterial virulence through mediating the nuclear trafficking of bacterial TALEs within plant cells.

To verify this hypothesis, we analyzed the effects of clustered regularly interspaced short palindromic repeats (CRISPR)–CRISPR-associated 9 (Cas9)-edited *OsIMPα1a* and *OsIMPα1b* on rice growth and bacterial virulence, and the results showed that OsIMPα1a is vital to rice, while OsIMPα1b has a crucial role in plant growth and development. We present evidence that OsIMPα1b is required for PthXo1 and TALI to move into rice cell nuclei to fulfil their virulence functions.

Results

OsIMPα1a and OsIMPα1b interact with PthXo1 through the AC motif

We initiated this study in 2015, at which point no plant importins had been determined to be related to bacterial TALEs. We retrieved the sequences of 16 *OsIMP* genes from rice genome annotation databases (Additional file 1: Table S1) but cloned only 10 *OsIMP*s from the rice variety Nipponbare (Fig. 1a). The OsIMPs were subjected to split-ubiquitin-based yeast two-hybrid (SUB-Y2H) assays together with PthXo1ΔN152 which lacks the first 152 amino acids at N-terminal (Fig. 1a). This modification was shown to prevent PthXo1 from autoactivation in SUB-Y2H assays performed previously (Yuan et al. 2016) and in the present study (Fig. 1b inset).

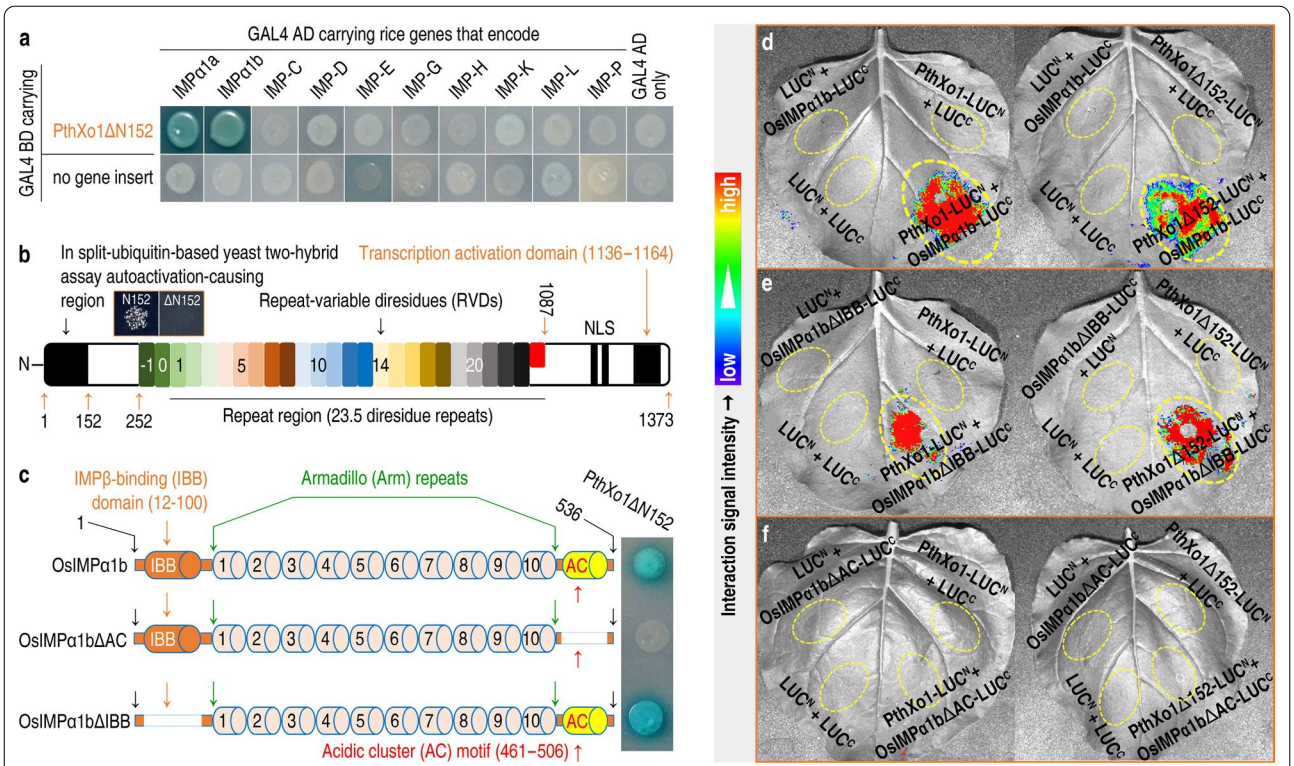

Fig. 1 OsIMPα1a and OsIMPα1b interact with PthXo1. **a** OsIMPα1a and OsIMPα1b were identified as interactors of PthXo1 in split-ubiquitin-based yeast two-hybrid (SUB-Y2H) assays of PthXo1 in combination with each of the indicated IMPs from rice. The protein–protein interactions were detected by an X-Gal assay of colonies grown on synthetic dropout (SD)-amino acid tryptophan-leucine nutrient (SD-WL) media. **b** Diagram of PthXo1 structural components, including the 152-amino acid-long N-terminal sequence, which is responsible for autoactivation of the protein. The inset shows the presence and absence of colonies growing on SD-tryptophan-leucine-alanine-histidine (SD-WLAH) medium from yeast cultures that produce full-length PthXo1 protein or the PthXo1Δ152 variant lacking the first 152 amino acids. **c** An additional SUB-Y2H assay revealed acidic cluster (AC) motif, instead of IMPβ-binding (IBB) domain, as a recognition motif driving the interactions of OsIMPα1a and OsIMPα1b with PthXo1. In **a** and **c**, each colony represents 9 colonies investigated in 3 experimental replicates. **d–f** Luciferin (Luc) living fluorescence imaging (LLFI) assays performed on *Nicotiana benthamiana* leaves transformed with each pair of the indicated proteins. Luc^N and Luc^C represent the N-terminal and C-terminal halves of Luc fusion constructs of each tested proteins. Each leaf image represents 12 leaves of 6 plants tested in 3 experimental replicates

Our SUB-Y2H assays clearly revealed direct interactions of PthXo1ΔN152 with OsIMPα1a or OsIMPα1b (Fig. 1a) but not for multiple pairs of control proteins (Fig. 1a and Additional file 2: Figure S1a). PthXo1 has been thoroughly demonstrated to have structural features (Fig. 1b) that meet functional requirements (Boch et al. 2009; Deng et al. 2012; Mak et al. 2012), especially the C-terminal NLS that determines its interactions with OsIMPα1a and OsIMPα1b (Hui et al. 2019). The results of our SUB-Y2H assays indicated that the interactions of OsIMPα1a and OsIMPα1b with PthXo1 were determined by the AC motif present in the C-terminal region of both OsIMPα1 sequences (Fig. 1c and Additional file 2: Figure S1a). In contrast, the N-terminal IBB domain was not involved in the interactions between OsIMPα1a/OsIMPα1b and PthXo1 (Fig. 1c and Additional file 2: Figure S1a).

These results were confirmed by luciferin (Luc) living fluorescence imaging (LLFI) assays performed on *Nicotiana benthamiana* leaves (Fig. 1d–f and Additional file 2: Figure S1b). LLFI assay confirmed the direct interaction between OsIMPα1a and PthXo1 (Additional file 2: Figure S1b). It further revealed that PthXo1ΔN152 resembled PthXo1 in terms of its ability to bind to OsIMPα1b (Fig. 1d) and that the ability of OsIMPα1bΔIBB (OsIMPα1b lacking the IBB motif) to interact with PthXo1 was similar to that of OsIMPα1b (Fig. 1e). Conversely, OsIMPα1bΔAC (OsIMPα1b lacking the AC motif) failed to interact with PthXo1 or PthXo1ΔN152 (Fig. 1f). Taken together, these results suggest that OsIMPα1a and OsIMPα1b interact with PthXo1 in a manner dependent on the AC motif, which is important for IMPα to efficiently function in nucleocytoplasmic trafficking (Miyamoto et al. 2016; Lüdke et al. 2021).

CRISPR/Cas9-based disruption of the *OsIMPα1a* gene in rice plants is embryo-lethal

To determine whether OsIMPα1a and OsIMPα1b are related to bacterial TALE translocation, both *OsIMPα1* genes were edited by the use of the CRISPR/Cas9-based gene editing technique. A single guide RNA (sgRNA) motif linked to the Cas9-recognizable protospacer adjacent motif (PAM) consisting of NGG was designed to target the *OsIMPα1a* complementary DNA strand at sites 212–234 and 315–336 in the first exon (Additional file 2: Figure S2a). The sgRNA, PAM, and NGG fusion constructs were introduced into the Nipponbare rice genome through *Agrobacterium*-mediated genetic transformation of embryo-derived callus with the recombinant plant binary vector pYLCRISPR/Cas9P_{Ubi}-H, which harbors *Cas9* and the hygromycin resistance gene *Hyg*, in addition to sgRNA (Ma et al. 2015). In total, 41 transgenic rice lines designated #1 to #41 were obtained from independent calli. According to Sanger sequencing-based genotyping, 7 transgenic lines were identified as having nucleotide mutations, including deletions and additions. Among them, 2 mutants were heterozygous and 5 mutants were homozygous (Additional file 1: Table S2).

These transgenic lines were designated *OsIMPα1a*-edited (*OsIMPα1a*-ED) lines *OsIMPα1a*-ED#2, *OsIMPα1a*-ED#4, *OsIMPα1a*-ED#14, *OsIMPα1a*-ED#17, *OsIMPα1a*-ED#21, OsIMPα1a-ED#32, and *OsIMPα1a*-ED#39 in accordance with the original codes of the independent T0 callus lines (Additional file 1: Table S2). The two homozygous T0 callus lines (*OsIMPα1a*-ED#2 and *OsIMPα1a*-ED#4) were lethal, as the embryos ultimately failed to produce progeny. T1 progeny of the three heterozygous T0 callus lines (*OsIMPα1a*-ED#14, *OsIMPα1a*-ED#21, and *OsIMPα1a*-ED#39) were further investigated and compared with the wild-type (WT) plants. We found that all the *OsIMPα1a*-ED#14, *OsIMPα1a*-ED#21, and *OsIMPα1a*-ED#39 lines were inferior to the WT plants in terms of seed germination and seedling growth (Additional file 2: Figure S2b, c). Although the WT seedlings grew well, the T1 embryos of the *OsIMPα1a*-ED#14, *OsIMPα1a*-ED#21, and *OsIMPα1a*-ED#39 seedlings did not survive during germination (Additional file 2: Figure S2c). Indeed, the T1 seedlings of these three lines died quickly after cotyledon stratification from the soil (Additional file 2: Figure S2c). Clearly, *OsIMPα1a* is critical for plant viability.

OsIMPα1b is an integral component of plant growth and development

The Nipponbare rice *OsIMPα1b* gene was also edited with the method similar to that used for editing of *OsIMPα1a*. A sgRNA motif linked to the PAM was designed to target the *OsIMPα1b* complementary genomic DNA strand at sites 203–225 and 505–527 in the first and second exons, respectively (Fig. 2a). The sgRNA-PAM fusion construct and the *Cas9* and *Hyg* genes were concomitantly introduced into the Nipponbare genome with the aid of a plant binary vector based on T-DNA construction (Ma et al. 2015). In total, 45 transgenic rice lines (#1 to #45) were obtained from independent calli. Based on genotyping by Sanger sequencing, five independent T0 mutant lines (*OsIMPα1b*-ED#6, *OsIMPα1b*-ED#17, *OsIMPα1b*-ED#26, *OsIMPα1b*-ED#29, and *OsIMPα1b*-ED#42) were identified as having nucleotide changes, including deletions and additions (Fig. 2b and Additional file 1: Table S2). All the five mutant lines were heterogeneous and had no random insertions or deletions. Despite evidently impaired seed germination (Additional file 2: Figure S2b), all these mutant lines were

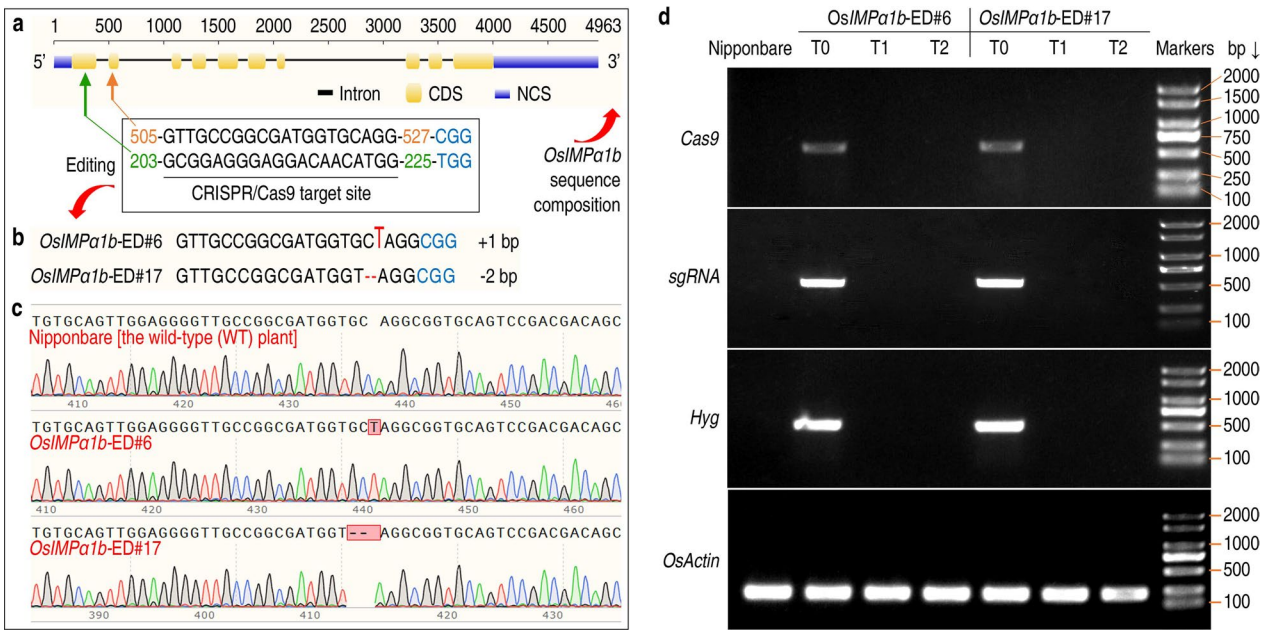

Fig. 2 CRISPR/Cas9-based *OsIMPα1b* gene editing and removal of transgenes by genetic segregation. **a** *OsIMPα1b* structural features along with the Cas9-targeting sites based on the T-DNA construction of an sgRNA motif linked to the Cas9-recognizable PAM consisting of NGG (CGG here). **b** Nucleotide changes in the targeting sequences of the *OsIMPα1b*-edited (*OsIMPα1b*-ED) T0 lines *OsIMPα1b*-ED#6 and *OsIMPα1b*-ED#17, both of which were further investigated. **c** Partial fragment sequences of *OsIMPα1b* in WT plants (rice variety Nipponbare) and T1 progenies of the *OsIMPα1b*-ED#6 and *OsIMPα1b*-ED#17 mutants. **d** Genetic segregation in which the transgenes were removed during the generation of T1 and T2 progenies of both mutants tested in comparison with the WT plants. The transgenes were analyzed via PCR using genomic DNA extracted from the corresponding plant templates, and the housekeeping gene *OsActin* was used as a reference. Each electrophoretic agarose image is representative of 3 experimental replicates

able to produce progeny (Fig. 3 and Additional file 2: Figures S2–S4).

T1 progenies of the *OsIMPα1b*-ED#6 and *OsIMPα1b*-ED#17 mutant lines were genotyped to identify the individuals that segregated away from the T-DNA (Fig. 2c). Plant DNA amplification by PCR in which primers specific to *Cas9*, *sgRNA*, or *Hyg* were used to identify T1 individuals that lack the transgene owing to genetic segregation (Fig. 2d). Moreover, Sanger sequencing revealed that some plants (*OsIMPα1b*-ED#6 and *OsIMPα1b*-ED#17) were homozygous (T2 progenies similar to their T1 counterparts) (Fig. 2d), which were used for further studies.

We determined that *OsIMPα1b* played a critical role in rice growth and development. Both the *OsIMPα1b*-ED#6 and *OsIMPα1b*-ED#17 mutant lines were much inferior to the WT plants in terms of embryo development, as indicated by impaired seed germination and seedling growth (Additional file 2: Figure S2b). These two mutants were also inferior to the WT plants in terms of vegetative growth and grain production (Fig. 3a and Additional file 2: Figure S3). In contrast to the WT, *OsIMPα1b*-ED#6 and *OsIMPα1b*-ED#17 presented considerable reductions in all quantitative growth parameters, such as plant height, plant fresh weight, and tiller number (Fig. 3b). Similarly, grain production was also impaired in both mutants (Fig. 3c and Additional file 2: Figure S4). In the end, grain yield was substantially decreased in both *OsIMPα1b*-ED#6 and *OsIMPα1b*-ED#17 compared with that of the WT plants (Fig. 3d). Clearly, *OsIMPα1b* gene disruption impaired rice growth, development, and grain production, suggesting that OsIMPα1b is an integral component of plant growth and development.

CRISPR/Cas9-based disruption of the *OsIMPα1b* gene results in the sequestration of TALEs from rice cell nuclei

PthXo1 and TALI produced by *Xoo* and *Xoc*, respectively, share highly conserved NLS (Fig. 4a), which determines TALE interactions with OsIMPα1a or OsIMPα1b (Szurek et al. 2001; Hui et al. 2019). Consistently, TALI was similar to PthXo1 in terms of the ability to bind to OsIMPα1a (Additional file 2: Figures S1b, S5) or OsIMPα1b (Figs. 1d, 4b), suggesting that the nuclear import of both TALEs may be subject to similar regulation by OsIMPα1b. To infer whether OsIMPα1b is related to the nuclear import of PthXo1 in the susceptible rice variety Nipponbare, PthXo1-RFP and OsIMPα1b-CFP fusion constructs were produced independently and concomitantly

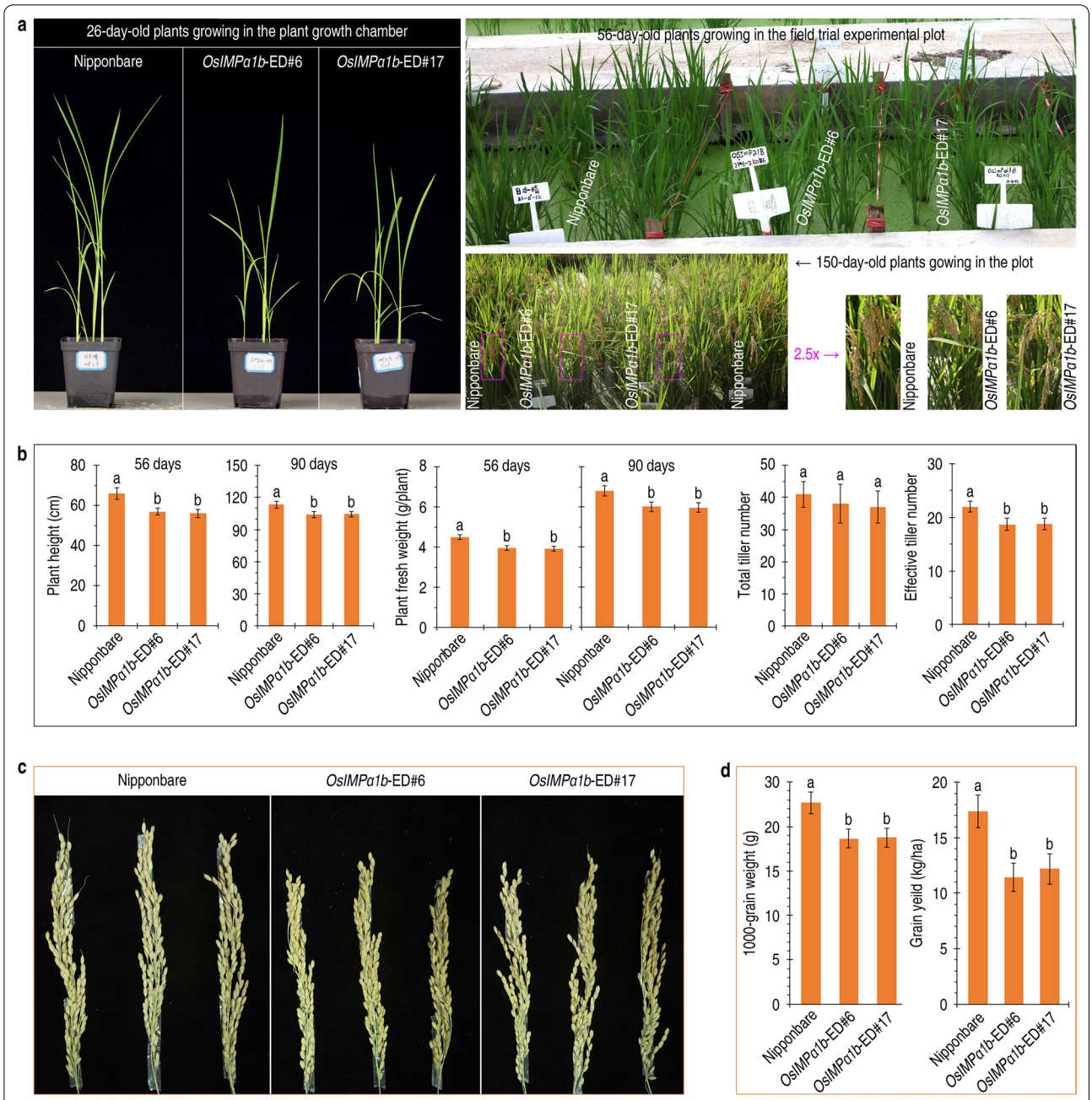

Fig. 3 Imaging and quantitative data showing growth and development differences between the WT plants and *OsIMPα1b*-edited (*OsIMPα1b*-ED) lines. **a** Plants in a growth chamber and in a specific pond within the experimental field. The image represents plant populations in approximately 1/15 hectare (1 Mu or 667 m^2) for each genotype. **b** Plant height and fresh weight of 56-day-old and 90-day-old plants and tiller number at the heading stage. The data shown are mean values ± standard deviations (SD) ($n = 3$). **c** Three spikelets in a row excised from different rice genotypes and representing grain production in approximately 1/15 hectare (1 Mu or 667 m^2) for each genotype. **d** Grain weight empirically determined in three experimental ponds and grain yield surveyed in 1/15 hectare (1 Mu or 667 m^2) divided into the three experimental ponds. The data shown are mean values ± standard deviations (SD) ($n = 3$). In **b** and **d**, different letters on bar graphs indicate significant differences among different plants based on Duncan's new multiple range test ($P < 0.05$)

in Nipponbare protoplasts by transformation with the individual genes or both fusion constructs. Using laser scanning confocal microscopy (LSCM), we found the independently produced PthXo1-RFP and OsIMPα1b-CFP in the nucleus and cytoplasm, respectively (Additional file 2: Figure S6). However, when PthXo1-RFP and

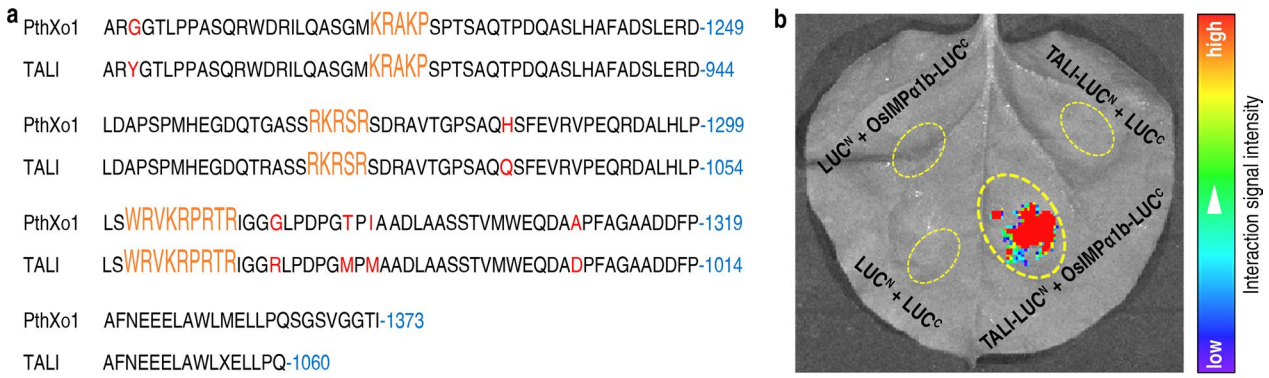

Fig. 4 Alignment of PthXo1 and TALI C-terminal sequences and luciferin (Luc) living fluorescence imaging (LLFI) assay of rice OsIMPα1a and *Xoc* TALI expressed in tobacco. **a** Sequence alignment highlighting the conserved consensus nuclear localization signals (NLSs) (taller orange letters) and highlighting differences in residues (in red). The conserved consensus NLSs were identified using the Clustal Omega program (https://www.ebi.ac.uk/Tools/msa/clustalo/). **b** LLFI assay representing 12 leaves of 6 tobacco plants

OsIMPα1b-CFP were expressed together, both proteins were colocalized to the nucleus (Additional file 2: Figure S6). Similarly, TALI-RFP and OsIMPα1b-CFP were localized to the nucleus and cytoplasm, respectively, when they were produced independently, but were colocalized to the nucleus when coexpressed (Additional file 2: Figure S7).

This hypothesis was verified by determining the subcellular localization of PthXo1 and TALI in the protoplasts of the WT and *OsIMPα1b*-ED#6 plants. Based on LSCM, the PthXo1-RFP fusion protein was localized to the nucleus of WT but in the cytoplasm of *OsIMPα1b*-ED#6 (Fig. 5a). Immunoblotting (IB) analyses revealed that the PathXo1-HA fusion protein was abundant in the nuclear fraction isolated from the WT plant protoplasts but was present at low levels in the nucleus of *OsIMPα1b*-ED#6 (Fig. 5b). Similarly, the TALI-RFP fusion protein was localized to the nucleus of WT but in the cytoplasm of *OsIMPα1b*-ED#6 (Fig. 5c). IB analyses revealed that the TALI-HA fusion protein was abundant in the nuclear fraction isolated from the WT plant protoplasts but was present at low levels in the nucleus of *OsIMPα1b*-ED#6 (Fig. 5d). In all the plants, neither PthXo1-HA nor TALI-HA was detected in the PM fractions (Fig. 5b, d). These results indicate that disruption of *OsIMPα1b* resulted in the sequestration of PthXo1 and TALI away from rice cell nuclei, suggesting that OsIMPα1b is required for both TALEs to be translocated into the nuclei of rice cells.

CRISPR/Cas9-based disruption of the *OsIMPα1b* gene suppresses *Xoo* virulence and promotes rice resistance to *Xoc*

In Nipponbare rice plants infected with the *Xoo* strain PXO99^{A}, the bacterial TALE PthXo1 induces virulence by activating its target gene *OsSWEET11* (Li et al. 2019; Chen et al. 2021) that determines host susceptibility and causes disease (Yang et al. 2006). Therefore, we hypothesized that the translocation of PthXo1 into rice cell nuclei is a prerequisite for *OsSWEET11* expression and bacterial virulence. In good agreement with this hypothesis, a considerable amount of PthXo1 was translocated from *Xoo* (PXO99^{A}) bacteria into the nuclei of rice cells (Fig. 6a), which is consistent with the strong expression of *OsSWEET11* (Fig. 6b) in the WT plants. In this case, *Xoo* bacteria multiplied sufficiently, attaining high population numbers within three days in rice leaves (Fig. 6c). This resulted in the full development of BB in the following 10 days, manifested as a long leaf blight lesion (Fig. 6d) and severe symptoms (Fig. 6e). In contrast to the WT plants, the *OsIMPα1b*-ED#6 and *OsIMPα1b*-ED#17 mutants coincidently presented greater reductions in PthXo1 translocation (Fig. 6a), *OsSWEET11* expression levels (Fig. 6b), and in planta bacterial populations (Fig. 6c). In the end, leaf blight lesion length (Fig. 6d) and symptoms (Fig. 6e) were considerably less severe in both mutants compared with the WT plants. Based on these results and those of the analyses described above, we propose that disruption of *OsIMPα1b* resulted in the suppression of *Xoo* virulence through sequestration of PthXo1 from cell nuclei of rice plants.

In Nipponbare plants infected with the *Xoc* strain GD41, the bacterial effector TALI induces virulence by suppressing plant defense responses, which essentially involve the expression of defense response genes (Chen et al. 2021; Long et al. 2021). Therefore, we hypothesized that the translocation of TALI into rice cell nuclei is a prerequisite for suppressing the expression of genes involved in the defense response and for rice resistance to BLS. In support of this hypothesis, substantial transport of TALI from *Xoc* (GD41) bacterial cells into rice cell

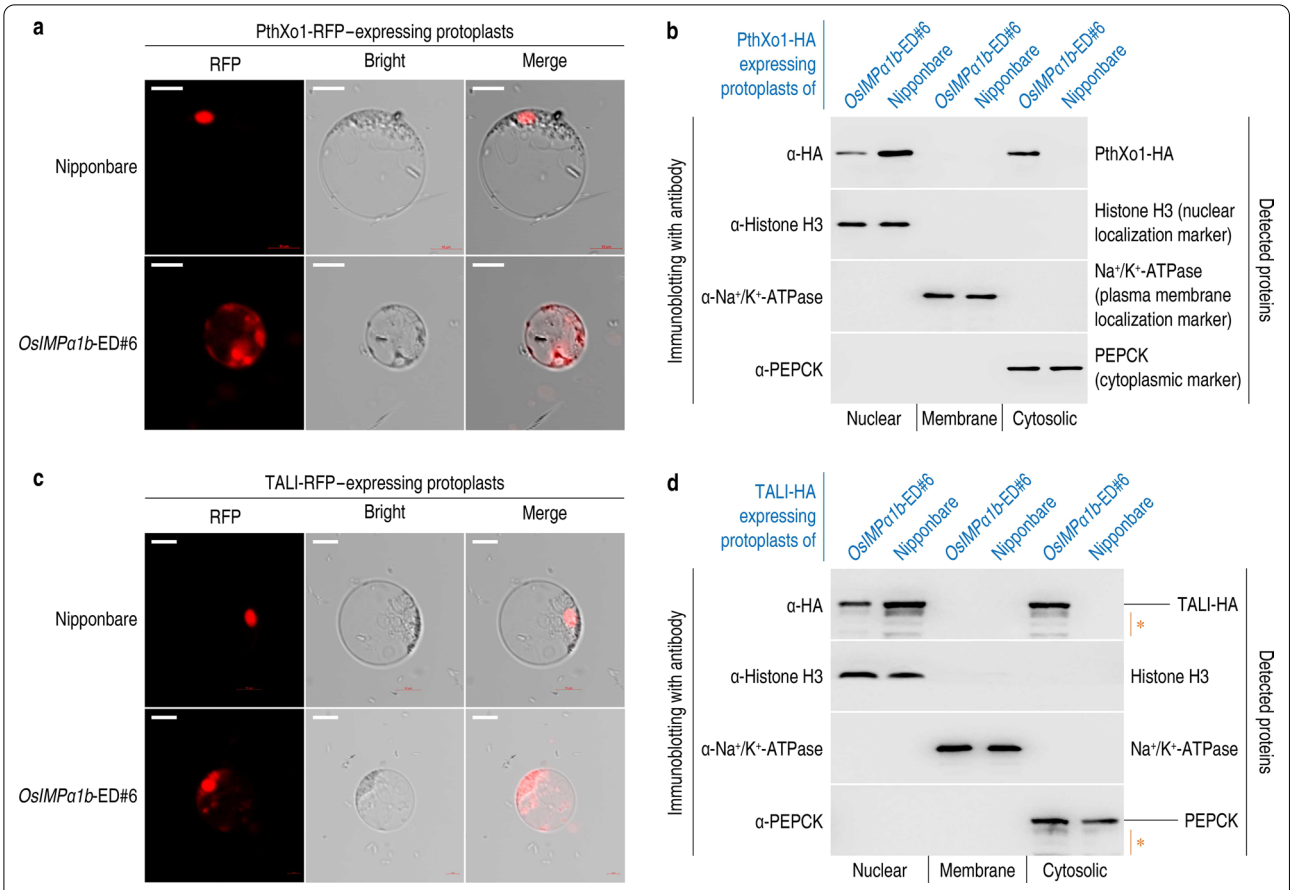

Fig. 5 Protoplast fluorescence images and Immunoblotting (IB) analyses showing differences in subcellular localization of the TALEs between the WT (Nipponbare) and *OsIMPα1b*-ED#6 plants. **a** Laser scanning confocal microscopy (LSCM) images of the plant protoplasts at 16 h after transformation with the *pthXo1-RFP* fusion gene. Each image is representative of 200–300 protoplasts. **b** IB of proteins extracted from protoplasts equivalent to those in **a**. **c** LSCM images of the plant protoplasts at 16 h after transformation with the *TALI-RFP* fusion gene. In **a** and **c**, each image is representative of 200–300 protoplasts; scale bars = 10 μm. **d** IB of proteins extracted from protoplasts equivalent to those in **c**. The asterisks and vertical lines indicate unidentified cross-reactive proteins

nuclei (Fig. 7a) concurrent with weak expression of the rice defense response genes *PR1a*, *PR5*, *PR10*, and *GSL12* (Fig. 7b) was detected in the WT plants. Consistently, *Xoc* bacteria sufficiently multiplied, resulting in a large bacterial population within three days in rice leaves (Fig. 7c). In the subsequent 7 days, severe BLS signs were observed on leaves of the WT plants (Fig. 7d). In contrast to the WT plants, the *OsIMPα1b*-ED#6 and *OsIMPα1b*-ED#17 mutants presented considerably less TALI translocation (Fig. 7a) and smaller in planta bacterial populations (Fig. 7c). In addition, in contrast to the WT plants, the *OsIMPα1b*-ED#6 and *OsIMPα1b*-ED#17 mutants exhibited greatly increased expression levels of *PR1a*, *PR5*, *PR10*, and *GSL12* (Fig. 7b). Ultimately, BLS symptom severity and lesion length were considerably alleviated in both the mutants compared with the WT plants (Fig. 7d). Evidently, disruption of *OsIMPα1b* resulted in the activation rather than suppression of rice defense responses to inhibit *Xoc* virulence.

OsIMPα1b disruption results in the promotion of pattern-triggered immunity (PTI)

As one of the *OsIMPα1b*-inhibited defense response genes (Fig. 7b), *GSL12* encodes the β-glucan synthetase-like (GSL) protein GSL12, which contributes to callose deposition on plant surfaces (Fu et al. 2014; Malinovsky et al. 2014; Zhai et al. 2017). Callose deposition is a conserved defense response against pathogen, insect attack, and other biotic stresses (Fu et al. 2014; Malinovsky et al. 2014; Zhai et al. 2017). In particular, *GSL12* expression and callose deposition also occur as downstream responses of the PTI pathway (Malinovsky et al. 2014; Chen et al. 2021). Based on these results, we hypothesized that *OsIMPα1b* might be related to PTI, the innate immunity activated by pathogen-associated molecular

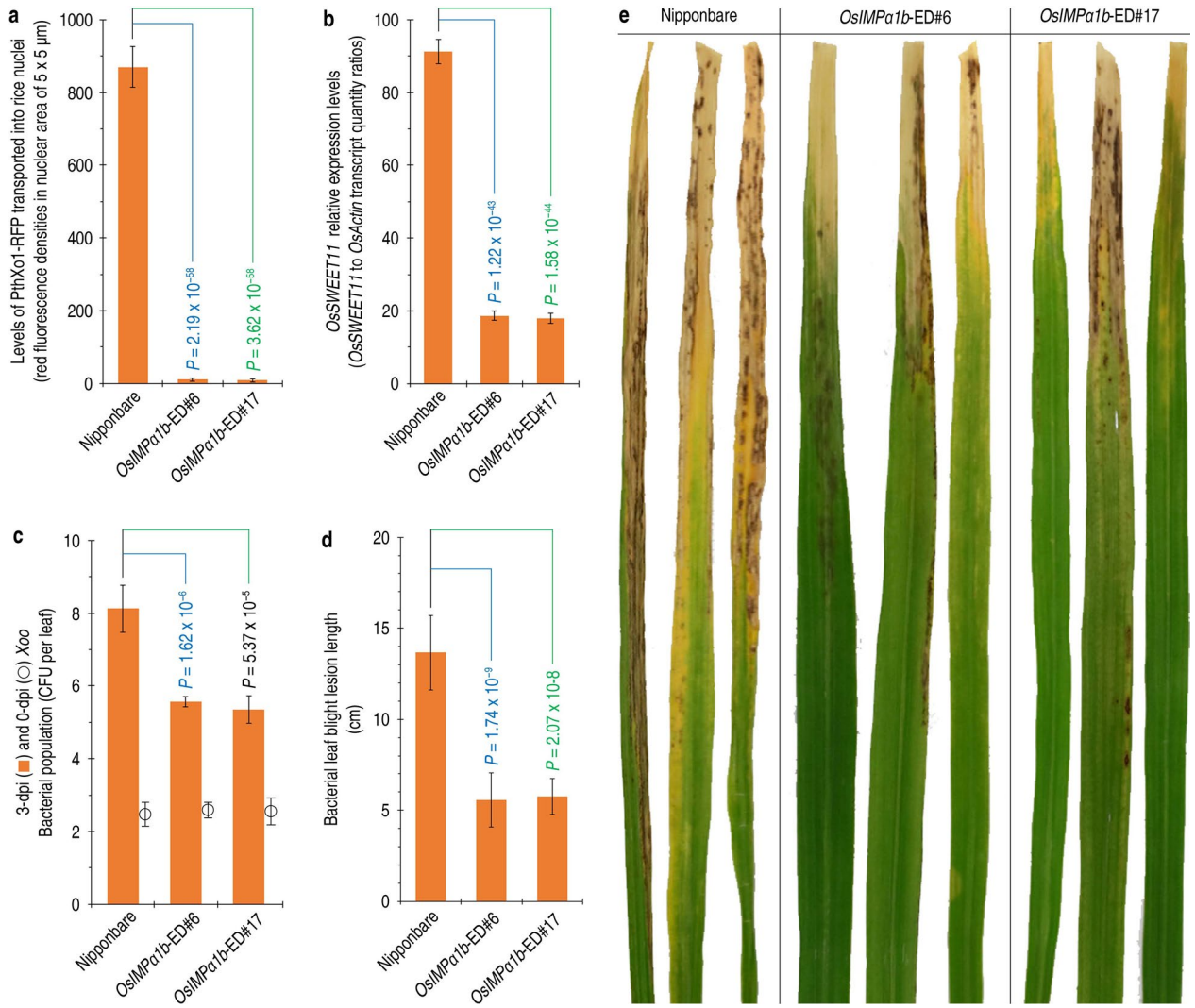

Fig. 6 Effects of PthXo1 translocation on *Xoo* virulence. **a**–**d** Comparisons of the *Xoo* virulence on the WT plants and *OsIMPα1b*-edited (*OsIMPα1b*-ED) mutants. PthXo1 translocation at 9 h post-inoculation (hpi) (**a**), expression of the PthXo1-targeted *OsSWEET11* gene at 24 hpi (**b**), in planta bacterial populations at 0 and 72 hpi (**c**), and disease severity at 14 days post-inoculation (dpi) (**d**) were determined correspondingly. The data shown are mean values ± SDs ($n = 3$). The *P* values are from two-sided unpaired Student's *t* tests ($P < 0.01$). **e** Fragments of *Xoo*-inoculated leaves imaged at 10 dpi. The leaf images are representative of 30 leaves of 15 plants tested in 3 experimental replications per genotype (WT, *OsIMPα1b*-ED#6, or *OsIMPα1b*-ED#17)

patterns (PAMPs) such as bacterial flagellin (Zipfel et al. 2004).

In support of this hypothesis, after editing the *OsIMPα1b* gene, we determined that critical PTI responses were promoted considerably (Fig. 8). The *OsIMPα1b*-ED#6 and *OsIMPα1b*-ED#17 mutant plants greatly exceeded the WT plants in terms of the extent of callose deposition on the surface of their leaves following exogenous application of flg22 (Fig. 8a), a PAMP functional fragment (Asai et al. 2002). Both mutants were more effective than the WT in supporting the induction effect of flg22 on the expression of the PTI regulatory genes *MPK3* and *MPK6* (Fig. 8b). Following flg22 application, moreover, several PTI response genes (*WRKY70*, *NHL10*, *PHI1-1*, and *GSL12*) were expressed at higher levels in both the *OsIMPα1b*-ED#6 and *OsIMPα1b*-ED#17 mutants than in the WT plants (Fig. 8b). Evidently, *OsIMPα1b* gene editing resulted in the promotion of the PTI pathway.

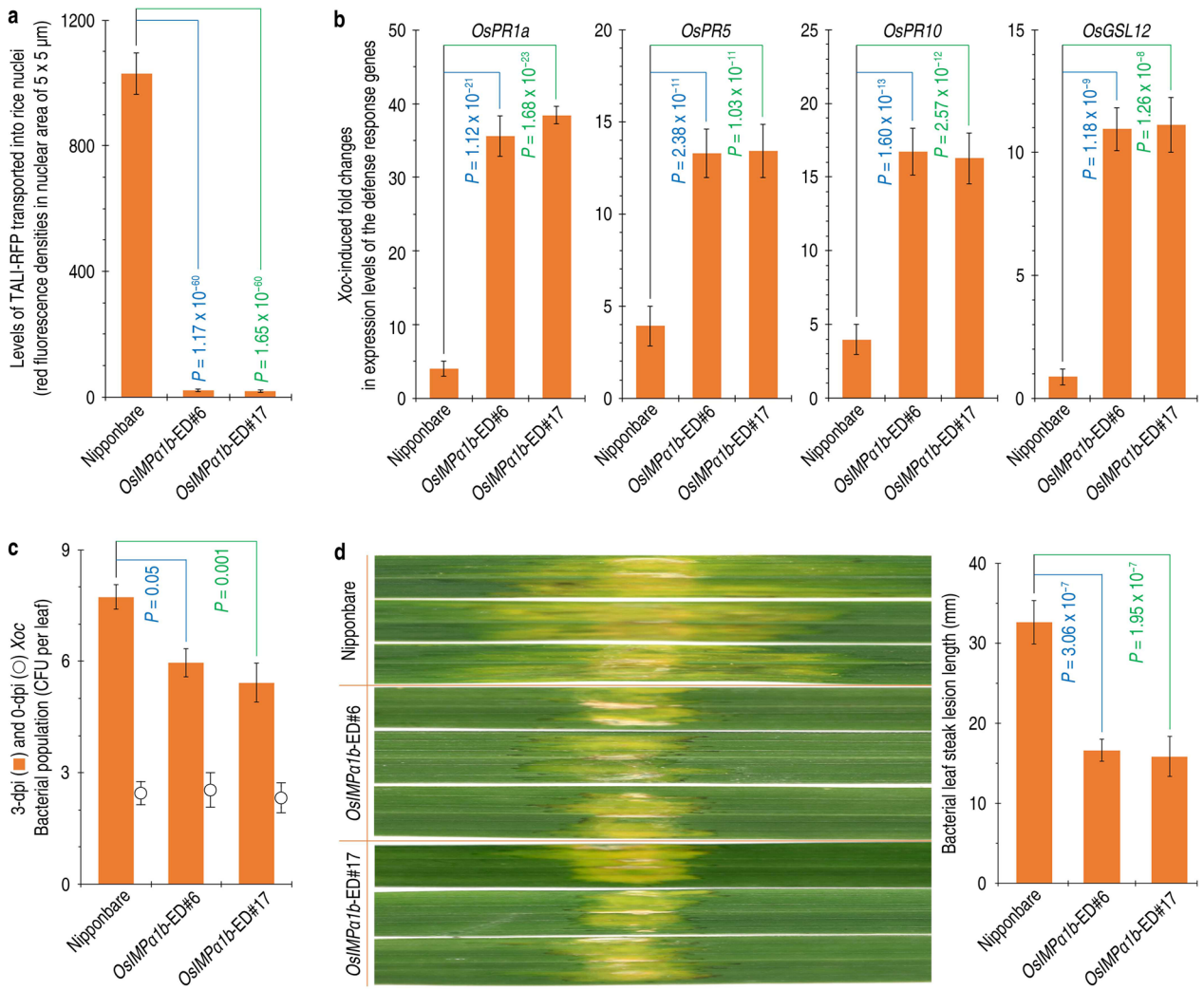

Fig. 7 Effects of TALI translocation into the nuclei of rice cells on the expression of genes involved in the rice defense response and *Xoc* virulence. TALI localization to rice cell nuclei at 9 h post-inoculation (hpi) (**a**), expression of rice defense response genes at 24 hpi (**b**), in planta bacterial populations at 0 and 72 hpi (**c**), and disease severity at 10 days post-inoculation (dpi) (**d**) were determined. The data shown are mean values ± SDs ($n = 3$). The *P* values are from two-sided unpaired Student's *t* tests ($P < 0.01$). In **d**, the leaf images are representative of 30 leaves of 15 plants tested in 3 experimental replications per genotype (WT, *OsIMPα1b*-ED#6, or *OsIMPα1b*-ED#17)

Discussion

This study was conceived to bridge the pivotal research gap concerning the in planta nucleocytoplasmic linkage found in the process of bacterial T3 effector translocation (Zhang et al. 2019a). We chose to test the specific hypothesis that OsIMPα1a and OsIMPα1b might facilitate bacterial virulence by mediating the nuclear trafficking of bacterial TALEs within plant cells (Hui et al. 2019). The importance of verifying this hypothesis has been increasingly highlighted by recent studies on bacterial T3 effector translocation (Ji and Dong 2015; Zhang et al. 2019a; Chen et al. 2021). It has been demonstrated that T3 effectors, including TALEs and nTALEs, secreted by plant pathogenic bacteria are translocated into plant cells to execute their virulence or avirulence functions, which depends on plant species and variety (Wang et al. 2018; Bian et al. 2019; Li et al. 2019; Mo et al. 2020; Chen et al. 2021). Both TALEs and nTALEs are translocated by bacterial T3 translocators (Ji and Dong 2015; Zhang et al. 2019a, b) and their receptors in the PMs of host plants (Wang et al. 2018; Bian et al. 2019; Li et al. 2019; Mo et al. 2020; Chen et al. 2021). Nevertheless, how TALEs further move into the nucleus has been not known until the present study.

In this study, we investigated the rice importins OsIMPα1a and OsIMPα1b, and three major results were

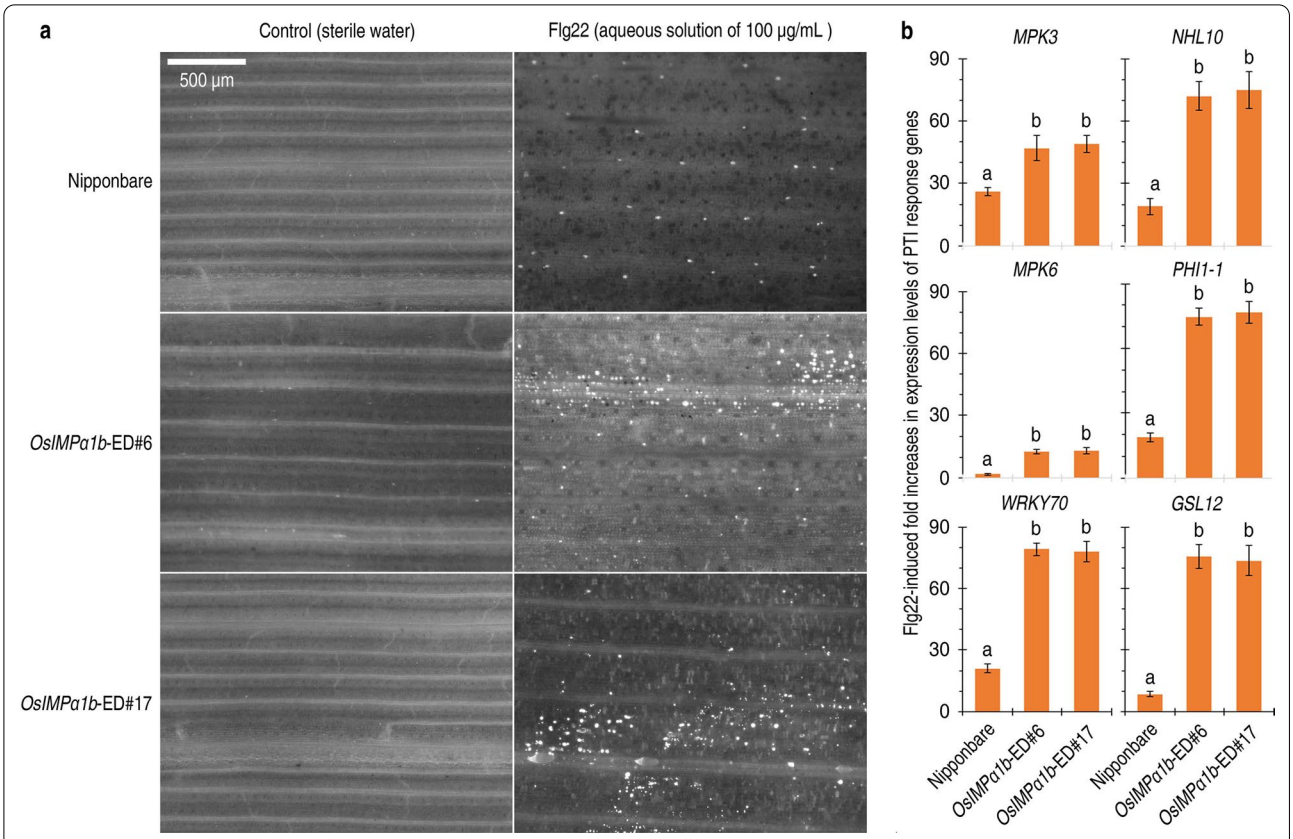

Fig. 8 Essential pattern-triggered immunity (PTI) responses occurred in leaves of the WT and *OsIMPα1b*-edited plants treated by spraying the tops of the plants with sterile water (control) or an aqueous solution of flg22. **a** Callose deposition on leaf surfaces of the different plants at 24 h after treatment. Each leaf image is representative of 15 leaves of 3 plants tested in 3 experimental replications. **b** Flg22-induced fold increases in foliar expression of rice PTI regulatory genes (*MPK3* and *MPK6*) and rice PTI response genes (*WRKY70*, *NHL10*, *PHI1-1*, and *GSL12*). The expression levels of the PTI regulatory and response genes were determined at 1 and 24 h after treatment. The data shown are mean values ± SDs ($n = 3$). The different letters on bar graphs indicate significant differences among different plants based on Duncan's new multiple range test ($P < 0.01$)

discovered. First, both OsIMPα1a and OsIMPα1b interact with the TALEs PthXo1 (Fig. 1 and Additional file 2: Figure S1) and TALI (Fig. 4b and Additional file 2: Figure S5) from *Xoo* and *Xoc*, respectively, on the basis of the identical NLSs present in both TALEs (Fig. 4a). We found that OsIMPα1b interacts with PthXo1 via the AC motif present in the C-terminal region (Fig. 1). Similarly, a recent study showed that PthXo1 depends on its NLS domain to interact with OsIMPα1a or OsIMPα1b and that both IMPs affect bacterial virulence (Hui et al. 2019). Nevertheless, whether OsIMPα1a and OsIMPα1b also affect bacterial effector translocation into rice cell nuclei were not determined. This possibility was found with respect to OsIMPα1–TALE interactions, for which there is a solid molecular basis concerning the interacting motifs (Fig. 1), and helps establish a molecular basis for bacterial effectors trafficking into rice cell nuclei to fulfil their virulence functions.

Second, we determined that OsIMPα1b is an integral component of rice growth and development and contributes considerably to rice grain production (Fig. 3 and Additional file 2: Figures S2–S4). Unfortunately, we have to reject further studies about *OsIMPα1a* owing to the embryo lethality of the *OsIMPα1a*-ED mutants (Additional file 2: Figure S2). At present, we do not know if and how the innate *OsIMPα1a* gene affects rice growth and development. We also do not know whether *OsIMPα1a* is related to bacterial virulence and effector translocation. These questions remain on hold until the embryo lethality of *OsIMPα1a*-ED mutants can be rescued.

Third, we presented evidence that, in rice, OsIMPα1b facilitates the translocation of the bacterial TALEs PthXo1 and TALI into the cell nucleus (Fig. 5 and Additional file 2: Figures S6, S7). Following nuclear import, both effectors execute their virulence functions (Chen et al. 2021; Long et al. 2021), possibly via different mechanisms, which were partially elucidated in the present study. In *Xoo*-infected *OsIMPα1b*-edited rice plants, OsIMPα1b sequesters PthXo1 from the nucleus,

the PthXo1-targeted host susceptibility rice gene (*OsSWEET11*) is no longer activated, and bacterial virulence and severity of BB disease are alleviated (Fig. 6). In *Xoc*-infected *OsIMPα1b*-edited rice plants, OsIMPα1b sequesters TALI from the nucleus, the function of TALI in suppressing rice defense responses (Long et al. 2021) is nullified, and rice defense responses are in turn activated to inhibit bacterial virulence and attenuate BLS severity (Fig. 7). These findings suggest that OsIMPα1b is a physiologically and pathologically relevant nuclear transport receptor with dual effects on plant growth and development and bacterial effector translocation.

In rice, the pathological function of OsIMPα1b affects at least two immunity pathways associated with the *Xoc* effector TALI (Figs. 7, 8). TALI has been shown to confer virulence to its host by suppressing systemic acquired resistance (SAR) and the expression of genes that are involved in the defense response and are characteristic of the SAR pathway in the susceptible rice variety Nipponbare (Long et al. 2021). As the defense response genes tested in the present study represent different immunity pathways, the expression of these genes indicated the activation of the corresponding immunity pathways. *PR1a*, *PR5*, and *PR10* encode the corresponding pathogenesis-related (PR) proteins that are associated with SAR (Boatwright and Pajerowska-Mukhtar 2013). Therefore, the *OsIMPα1b*-dependent *PR1a*, *PR5*, and *PR10* expression indicated that *OsIMPα1b* is related to the SAR pathway (Fig. 7b). Moreover, OsIMPα1b plays an important role in the PTI pathway (Fig. 8). Evidently, OsIMPα1b is associated with at least two cellular pathways that regulate innate immunity in rice. Presumably, some transcription factors involved in the innate immunity pathways are modulated by OsIMPα1b such that defense responses are regulated at the transcriptional level. Overall, characterizing the molecular mechanisms assumed to govern the functions of *OsIMPα1b* in the SAR and PTI pathways will be the subjects of future studies.

Conclusions

We have presented evidence demonstrating that OsIMPα1b is a physiologically and pathologically relevant nuclear transport receptor that has dual effects on plant growth and bacterial virulence. Rice OsIMPα1b interacting with the bacterial effectors PthXo1 and TALI represents a molecular basis on which plant importins transport bacterial effectors (TALEs) into the cell nucleus. This notion was confirmed by the LSCM and IB results showing that TALEs colocalized with OsIMPα1b in the nuclei of the WT plants, in contrast to the distribution of TALEs throughout the cytoplasm of the OsIMPα1b loss-of-function mutants. In *Xoo*-infected *OsIMPα1b*-edited rice plants, OsIMPα1b sequesters PthXo1 from the nucleus, the PthXo1 target gene *OsSWEET11* is no longer activated, and bacterial virulence and BB disease symptoms are ultimately alleviated. In *Xoc*-infected *OsIMPα1b*-edited rice plants, OsIMPα1b sequesters TALI from the nucleus, rice defense responses are no longer suppressed, and rice defense responses are therefore activated to inhibit bacterial virulence and reduce BLS severity.

Methods

Microbial materials and culture conditions

The *Xoo* strain PXO99^{A} and *Xoc* strain GD41 were cultured on nutrient broth (NB) or nutrient agar (NA) medium (Li et al. 2011). The *Agrobacterium tumefaciens* strain GV3101 was used in plant transformations and cultured on NB medium supplemented with kanamycin of 50 μg/mL and rifampicin of 20 μg/mL. The yeast (*Saccharomyces cerevisiae*) strain AH109 was used in SUB-Y2H (Dualsystems) assays and grown on synthetic dropout (SD)-amino acid nutrient medium. These microbes were cultured in incubators at 28 °C.

Plant materials and growth conditions

Seeds of rice (*O. sativa*) and tobacco (*N. benthamiana*) were maintained in our lab. Tobacco plants were grown in a greenhouse under regular conditions and used for LLFI assays. Rice seeds were germinated in flat plastic trays filled with the PINDSTRUP substrate (Pindstrup group). Three days later, the germinating seedlings were moved into 12-L pots (2–5 plants per pot) filled with the PINDSTRUP substrate. Seeds were germinated and plants were grown in environment-controlled chambers at 26 ± 1 °C, 12-h light at 250 ± 50 μmol quanta/(m^2.s) and a relative humidity of 85% except specified elsewhere. These rice plants were used in bacterial infection assessments and protoplast preparation. For growth and development assessments, nursery seedlings grown for 30 days in the plant growth chamber were transplanted into rice-growth ponds located at Panhe Campus of Shandong Agricultural University, Taian, Shandong Province, China.

Molecular interaction assays

SUB-Y2H (Li et al. 2015) and LLFI (Zhou et al. 2018) assays were performed as previously described.

Plant gene editing and mutant generation

Editing of rice importin genes (*OsIMPα1a* and *OsIMPα1b*) and subsequent generation of the *OsIMPα1a* or *OsIMPα1b* loss-of-function rice (Nipponbare) mutants were conducted by using the protocols described previously (Kuang et al. 2020). The pYLCRISPR/Cas9P_{Ubi}-H

binary vector was constructed as previously described (Ma et al. 2015). In brief, the nucleotide oligos (Additional file 1: Table S3) corresponding to the identified mutation regions of both *OsIMPα1s* were chosen and incorporated into the sgRNA expression vector (pYLgRNA). The resulting sgRNA expression cassettes were then shuttled into pYLCRISPR/Cas9P_{Ubi}-H through Gateway recombination (Ren et al. 2018). These constructs were introduced into Nipponbare genome by the conventional *Agrobacterium*-mediated transformation procedure. Sanger sequencing with gene-specific sequencing primers were performed to identify the editing-caused mutations and the homozygosity of the mutation (nucleotide change). T1 and T2 progenies of the mutant lines *OsIMPα1b*-ED#6 and *OsIMPα1b*-ED#17 were genotyped to identify the individuals in which the T-DNA was segregated out, and these plants were used in further studies.

Plant growth and development assessments

Rice growth and development were investigated in small-scale field trials conducted in rice-growing ponds. In China, the term 'Mu' has been conventionally used to specify the area of cultivated land, and 1 Mu is equivalent to 666.7 m^2 or 1/15 hectare. In Taian, a single field trial occupied 1/10 hectare (1.5 Mu) and was divided equally into three experimental plots. The WT, *OsIMPα1b*-ED#6, and *OsIMPα1b*-ED#17 plants were planted randomly into three plots. Rice growth was monitored. Plant weight and grain yield were surveyed.

Subcellular localization of proteins

Rice protoplasts were prepared from aerial parts of 20-day-old rice seedlings using a previously described protocol (Yoo et al. 2007). Protoplasts were transformed with *OsIMPα1b-CFP* alone or in combination with *pthXo1-RFP* and *TALI-RFP*, respectively, using the polyethyleneglyco-mediated method (Zhang et al. 2011). Approximate 16 h later, transformed protocols were observed under a laser scanning confocal microscope (Zeiss LSM880). Excitation laser wavelengths of 470 nm and 563 nm were used to capture fluorescence signals of CFP and RFP, respectively. To carry out IB, proteins were isolated from the rice protoplasts at 16 h after transformation. Proteins present in the nucleus and associated with PMs were isolated using the Minute Plasma Membrane Protein Isolation Kit for Plants (Invent). Nuclear and membrane proteins were quantified using a BCA protein assay kit (TransGen Biotech) and then separated by electrophoresis using 10% SDS-PAGE gels. The target proteins were detected by hybridization with the corresponding antibodies, with rat-produced α-HA (TransGen Biotech) at a 5000-fold dilution, both rabbit-produced α-Histone H3 (PhytoAB Inc) and α-Na^+/K^+-ATPase (PhytoAB Inc) at a 2000-fold dilution, and secondary peroxidase-conjugated anti-mouse or anti-rabbit antibody (TransGen Biotech) at a 5000-fold dilution.

Bacterial infection assessments

Overnight bacterial cultures of *Xoo* and *Xoc* incubated on NA medium were washed twice and resuspended in sterile water to generate inoculum suspensions with an optical density of OD_{600} = 0.3. The *Xoo* suspension was amended with 0.03% v/v Silwet L-77, and the mixture was inoculated on leaves of 30-day-old rice plants by the leaf-clipping method (Kauffman et al. 1973). The *Xoc* suspension was directly inoculated on leaves of 2-week-old rice seedlings by infiltration with needleless syringes (Reimers et al. 1992) approximately at the central site. Infection degrees were evaluated by determining populations of bacteria multiplied in leaves and quantifying the subsequently formed symptoms. Bacteria multiplied in leaves were recovered, incubated on NA medium, quantified as colony formation unit (CFU), and presented as logarithmic CFU values per leaf. BB and BLS symptoms were scored by photographing or measuring lesion lengths and sizes in leaves at 14 and 10 dpi, respectively.

Gene expression analysis

Total RNA was isolated at 24 h after treatment with an RNAiso Plus reagent (Takara). RNA quantity and quality were evaluated using NanoDrop 8000 (Thermo Scientific). cDNA was prepared from equal amounts of total RNA per sample with the HiScript® II 1st Strand cDNA Synthesis Kit (Vazyme). Reverse transcription-quantitative PCR (RT-qPCR) experiments were conducted on ABI QuantStudio 3 (Thermo Fisher) using ChamQ™ Universal SYBR® qPCR Master Mix (Vazyme). All the RT-qPCR experiments were performed using specific primers (Additional file 1: Table S3) with the constitutively expressed *OsActin* gene as a reference (Chen et al. 2021). Relative expression level of a gene tested was quantified as the transcript quantity ratio to *OsActin*.

Callose deposition assay

Leaves of 2-week-old rice seedlings were sprayed with flg22 (GeneScript) or sterile H_2O containing 0.03% v/v Silwet L-77. Callose deposition was detected at 24 h after treatment as described previously (Yang et al. 2019).

Statistical analysis

Significance in differences between (among) data from different plants (genotypes) or treatments were estimated by analysis of variance and student's *t*-tests or Duncan's new multiple range tests using GraphPad Prism 8.0 (https://www.graphpad.com/).

Abbreviations
AC: Acidic cluster; BB: Bacterial blight; BLS: Bacterial leaf streak; CFP: Cyan-fluorescent protein; CFU: Colony formation unit; GSL: β-Glucan synthetase-like; IBB: IMPβ-binding; IMP: Importin; LLFI: Luciferin living fluorescence imaging; LSCM: Laser scanning confocal microscopy; Luc: Luciferin; NLS: Nuclear localization signal; nTALEs: Non-TAL effectors; PAM: Protospacer adjacent motif; PM: Plasma membrane; PTI: Pattern-triggered immunity; RFP: Red-fluorescent protein; SAR: Systemic acquired resistance; sgRNA: Single guide RNA; TAL: Transcription activator-like; TALEs: Transcription activator-like effectors; X-Gal: 5-bromo-4-chloro-3-indolyl-β-D-galactopyranoside; *Xoc*: *Xanthomonas oryzae* pv. *oryzicola*; *Xoo*: *Xanthomonas oryzae* pv. *oryzae*; Xops: *Xanthomonas* outer proteins.

Supplementary Information

The online version contains supplementary material available at https://doi.org/10.1186/s42483-022-00149-7.

Additional file 1. **Table S1.** Rice importins retrieved from Rice Genome Annotation Project databases. **Table S2.** Early characterizations of *OsIMPα1a*-edited (*OsIMPα1a*-ED) and *OsIMPα1b*-edited (*OsIMPα1b*-ED) rice lines. **Table S3.** Information on genes tested and primers used in this study.

Additional file 2. **Figure S1**. Split-ubiquitin-based yeast two-hybrid (SUB-Y2H) and luciferin (Luc) living fluorescence imaging (LLFI) assays of protein combinations between PthXo1 and different variants of OsIMPα1b and OsIMPα1a (shown as IMPα1b and IMPα1a in this figure). **Figure S2**. CRISPR/Cas9-based *OsIMPα1a* gene editing and viability of *OsIMPα1a*-edited (*OsIMPα1a*-ED) and *OsIMPα1b*-edited (*OsIMPα1b*-ED) rice lines. **Figure S3**. Plants growing in the specific rice-growing pond and representing plant populations of the wild type (Nipponbare) and *OsIMPα1b*-edited lines (*OsIMPα1b*-ED#6 and *OsIMPα1b*-ED#17). **Figure S4**. Seed-maturating plants from the specific rice-growth pond and the representing plant populations of the wild type (Nipponbare) and *OsIMPα1b*-edited lines (*OsIMPα1b*-ED#6 and *OsIMPα1b*-ED#17). **Figure S5**. Luciferin (Luc) living fluorescence imaging (LLFI) assays of rice OsIMPα1a and *Xoc* TALI concomitantly expressed in tobacco. **Figure S6.** Laser scanning confocal microscopy (LSCM) images of rice protoplasts at 16 h after individual or collective transformation with the *pthXo1-RFP* and *OsIMPα1b-CFP*. **Figure S7**. Laser scanning confocal microscopy (LSCM) images of rice protoplasts at 16 h after individual or collective transformation with *TALI-RFP* and *OsIMPα1b-CFP*.

Acknowledgements
We thank Prof. Huanbin Zhou (Institute of Plant Protection, Chinese Academy of Agricultural Sciences, Beijing, China) for the gene editing and mutant generation (accomplished in 2016). We thank Dr. Chenhao Li (the former doctoral student studying in our lab) for initiating this study (in 2015).

Authors' contributions
JP designed and performed the experiments, analyzed the data, and wrote the manuscript. JN, XC, LZ, XY, PL, and HS performed the experiments. CS and HD designed the experiments and wrote the manuscript. HD conceived the project and finalized the manuscript. All authors read and approved the final manuscript.

Funding
This study was supported by the National Natural Science Foundation of China (Grant numbers 31772247, 32072399, and 32170202) and the Natural Science Foundation of Shandong Province (ZR2020MC113, ZR2020MC120, and ZR2020QC126).

Availability of data and materials
Not applicable.

Declarations

Ethics approval and consent to participate
Not applicable.

Consent for publication
Not applicable.

Competing interests
The authors declare that they have no competing interests.

Author details
[1]College of Plant Protection, Nanjing Agricultural University, Nanjing 210095, China. [2]State Key Laboratory of Crop Biology, College of Plant Protection, Shandong Agricultural University, Taian 271018, China. [3]Qilu College, Shandong Agricultural University, Taian 271018, China. [4]Biotechnology College, Jiangsu University of Science and Technology, Zhenjiang 202100, China.

Received: 12 August 2022 Accepted: 14 November 2022
Published online: 25 November 2022

References

Asai T, Tena G, Plotnikova J, Willmann MR, Chiu WL, Gomez-Gomez L, et al. MAP kinase signalling cascade in *Arabidopsis* innate immunity. Nature. 2002;415:977–83. https://doi.org/10.1038/415977a.

Bergeron JRC, Marlovits TC. Cryo-EM of the injectisome and type III secretion systems. Curr Opin Struct Biol. 2022;75: 102403. https://doi.org/10.1016/j.sbi.2022.102403.

Bian H, Zhang L, Chen L, Wang W, Ji H, Dong H. Real-time monitoring of translocation of selected type-III effectors from Xanthomonas oryzae pv oryzae into rice cells. J Biosci. 2019;44:82. https://doi.org/10.1007/s12038-019-9916-0.

Boatwright JL, Pajerowska-Mukhtar K. Salicylic acid: an old hormone up to new tricks. Mol Plant Pathol. 2013;14:623–34. https://doi.org/10.1111/mpp.12035.

Boch J, Scholze H, Schornack S, Landgraf A, Hahn S, Kay S, et al. Breaking the code of DNA binding specificity of TAL-type III effectors. Science. 2009;326:1509–12. https://doi.org/10.1126/science.1178811.

Bogdanove AJ, Voytas DF. TAL effectors: customizable proteins for DNA targeting. Science. 2011;333:1843–6. https://doi.org/10.1126/science.1204094.

Bundalovic-Torma C, Lonjon F, Desveaux D, Guttman DS. Diversity, evolution, and function of *Pseudomonas syringae* effectorome. Annu Rev Phytopathol. 2022;60:211–36. https://doi.org/10.1146/annurev-phyto-021621-121935.

Büttner D. Protein export according to schedule: architecture, assembly, and regulation of type III secretion systems from plant- and animal-pathogenic bacteria. Microbiol Mol Biol Rev. 2012;76:262–310. https://doi.org/10.1128/MMBR.05017-11.

Büttner D, Bonas U. Port of entry–the type III secretion translocon. Trends Microbiol. 2002;10:186–92. https://doi.org/10.1016/s0966-842x(02)02331-4.

Büttner D, Nennstiel D, Klusener B, Bonas U. Functional analysis of HrpF, a putative type III translocon protein from *Xanthomonas campestris* pv. *vesicatoria*. J Bacteriol. 2002;184:2389–98. https://doi.org/10.1128/JB.184.9.2389-2398.2002.

Chang CW, Couñago RL, Williams SJ, Bodén M, Kobe B. Crystal structure of rice importin-α and structural basis of its interaction with plant-specific nuclear localization signals. Plant Cell. 2012;24:5074–88. https://doi.org/10.1105/tpc.112.104422.

Chang CW, Williams SJ, Couñago RM, Kobe B. Structural basis of interaction of bipartite nuclear localization signal from *Agrobacterium* VirD2 with rice importin-α. Mol Plant. 2014;7:1061–4. https://doi.org/10.1093/mp/ssu014.

Chen X, Ma J, Wang X, Lu K, Liu Y, Zhang L, et al. Functional modulation of an aquaporin to intensify photosynthesis and abrogate bacterial virulence in rice. Plant J. 2021;108:330–46. https://doi.org/10.1111/tpj.15427.

Deng D, Yan C, Pan X, Mahfouz M, Wang J, Zhu JK, et al. Structural basis for sequence-specific recognition of DNA by TAL effectors. Science. 2012;335:720–3. https://doi.org/10.1126/science.1215670.

Ems-McClung SC, Emch M, Zhang S, Mahnoor S, Weaver LN, Walczak CE. RanGTP induces an effector gradient of XCTK2 and importin α/β for spindle microtubule cross-linking. J Cell Biol. 2020;219: e201906045. https://doi.org/10.1083/jcb.201906045.

Fu M, Xu M, Zhou T, Wang D, Tian S, Han L, et al. Transgenic expression of a functional fragment of harpin protein Hpa1 in wheat induces the phloem-based defence against English grain aphid. J Exp Bot. 2014;65:1439–53. https://doi.org/10.1093/jxb/ert488.

Gaytán MO, Monjarás FJ, Soto E, Espinosa N, Benítez JM, Georgellis D, et al. Novel insights into the mechanism of SepL-mediated control of effector secretion in enteropathogenic *Escherichia coli*. MicrobiologyOpen. 2018;7: e00571. https://doi.org/10.1002/mbo3.571.

Goldfarb DS, Corbett AH, Mason DA, Harreman MT, Adam SA. Importin α: a multipurpose nuclear-transport receptor. Trends Cell Biol. 2004;14:505–14. https://doi.org/10.1016/j.tcb.2004.07.016.

Hajra D, Nair AV, Chakravortty D. An elegant nano-injection machinery for sabotaging the host: role of Type III secretion system in virulence of different human and animal pathogenic bacteria. Phys Life Rev. 2021;38:25–54. https://doi.org/10.1016/j.plrev.2021.05.007.

Hui S, Shi Y, Tian J, Wang L, Li Y, Wang S, et al. TALE-carrying bacterial pathogens trap host nuclear import receptors for facilitation of infection of rice. Mol Plant Pathol. 2019;20:519–32. https://doi.org/10.1111/mpp.12772.

Ji H, Dong H. Key steps in type III secretion system (T3SS) towards translocon assembly with potential sensor at plant plasma membrane. Mol Plant Pathol. 2015;16:762–73. https://doi.org/10.1111/mpp.12223.

Jiang CJ, Shoji K, Matsuki R, Baba A, Inagaki N, Ban H, et al. Molecular cloning of a novel importin α homologue from rice, by which constitutive photomorphogenic 1 (COP1) nuclear localization signal (NLS)-protein is preferentially nuclear imported. J Biol Chem. 2001;276:9322–9. https://doi.org/10.1074/jbc.M006430200.

Jo K, Kim EJ, Yu HJ, Yun CH, Kim DW. Host cell nuclear localization of *Shigella flexneri* effector OspF is facilitated by SUMOylation. J Microbiol Biotechnol. 2017;27:610–5. https://doi.org/10.4014/jmb.1611.11066.

Kauffman HE, Reddy APK, Hsieh SPY, Merca SD. An improved technique for evaluating resistance of rice varieties to *Xanthomonas oryzae*. Plant Dis Rep. 1973;57:537–41.

Kim JG, Li X, Roden JA, Taylor KW, Aakre CD, Su B, et al. *Xanthomonas* T3S effector XopN suppresses PAMP-triggered immunity and interacts with a tomato atypical receptor-like kinase and TFT1. Plant Cell. 2009;21:1305–23. https://doi.org/10.1105/tpc.108.063123.

Kuang Y, Li S, Ren B, Yan F, Spetz C, Li X, et al. Base-editing-mediated artificial evolution of *OsALS1 in planta* to develop novel herbicide-tolerant rice germplasms. Mol Plant. 2020;13:565–72. https://doi.org/10.1016/j.molp.2020.01.010.

Li Y, Che Y, Zou H, Cui Y, Guo W, Zou L, et al. Hpa2 required by HrpF to translocate *Xanthomonas oryzae* transcriptional activator-like effectors into rice for pathogenicity. Appl Environ Microbiol. 2011;77:3809–18. https://doi.org/10.1128/AEM.02849-10.

Li L, Wang H, Gago J, Cui H, Qian Z, Kodama N, et al. Harpin Hpa1 interacts with aquaporin PIP1;4 to promote the substrate transport and photosynthesis in *Arabidopsis*. Sci Rep. 2015;5:17207. https://doi.org/10.1038/srep17207.

Li P, Zhang L, Mo X, Ji H, Bian H, Hu Y, et al. Rice aquaporin PIP1;3 and harpin Hpa1 of bacterial blight pathogen cooperate in a type III effector translocation. J Exp Bot. 2019;70:3057–73. https://doi.org/10.1093/jxb/erz130.

Long J, Wang W, Chen X, Liu Y, Zhang M, Song C, et al. Identification of a TAL effector in *Xanthomonas oryzae* pv. *oryzicola* enhancing pathogen growth and virulence in plants. Physiol Mol Plant P. 2021;114:101620. https://doi.org/10.1016/j.pmpp.2021.101620.

Lüdke D, Rohmann PFW, Wiermer M. Nucleocytoplasmic communication in healthy and diseased plant tissues. Front Plant Sci. 2021;12: 719453. https://doi.org/10.3389/fpls.2021.719453.

Ma X, Zhang Q, Zhu Q, Liu W, Chen Y, Qiu R, et al. A robust CRISPR/Cas9 system for convenient, high-efficiency multiplex genome editing in monocot and dicot plants. Mol Plant. 2015;8:1274–84. https://doi.org/10.1016/j.molp.2015.04.007.

Mak AN, Bradley P, Cernadas RA, Bogdanove AJ, Stoddard BL. The crystal structure of TAL effector PthXo1 bound to its DNA target. Science. 2012;335:716–9. https://doi.org/10.1126/science.1216211.

Malinovsky FG, Fangel JU, Willats WG. The role of the cell wall in plant immunity. Front Plant Sci. 2014;5:178. https://doi.org/10.3389/fpls.2014.00178.

Merkle T. Nucleo-cytoplasmic partitioning of proteins in plants: implications for the regulation of environmental and developmental signalling. Curr Genet. 2003;44:231–60. https://doi.org/10.1007/s00294-003-0444-x.

Miyamoto Y, Yamada K, Yoneda Y. Importin α: a key molecule in nuclear transport and non-transport functions. J Biochem. 2016;160:69–75. https://doi.org/10.1093/jb/mvw036.

Mo X, Zhang L, Liu Y, Wang X, Bai J, Lu K, et al. Three proteins (Hpa2, HrpF and XopN) are concomitant Type III translocators in bacterial blight pathogen of rice. Front Microbiol. 2020;11:1601. https://doi.org/10.3389/fmicb.2020.01601.

Picking WD, Barta ML. The tip complex: from host cell sensing to translocon formation. In: Wagner S, Galan J, editors. Bacterial type III protein secretion systems. Cham: Springer; 2019. p. 173–99. https://doi.org/10.1007/82_2019_171.

Reimers PJ, Guo A, Leach JE. Increased activity of a cationic peroxidase associated with an incompatible interaction between *Xanthomonas oryzae* pv. *oryzae* and rice (*Oryza sativa*). Plant Physiol. 1992;99:1044–50. https://doi.org/10.1104/pp.99.3.1044.

Ren B, Yan F, Kuang Y, Li N, Zhang D, Zhou X, et al. Improved base editor for efficiently inducing genetic variations in rice with CRISPR/Cas9-guided hyperactive *hAID* Mutant. Mol Plant. 2018;11:623–6. https://doi.org/10.1016/j.molp.2018.01.005.

Roth C, Lüdke D, Klenke M, Quathamer A, Valerius O, Braus GH, et al. The truncated NLR protein TIR-NBS13 is a MOS6/IMPORTIN-α3 interaction partner required for plant immunity. Plant J. 2017;92:808–21. https://doi.org/10.1111/tpj.13717.

Santi-Rocca J, Blanchard N. Membrane trafficking and remodeling at the host-parasite interface. Curr Opin Microbiol. 2017;40:145–51. https://doi.org/10.1016/j.mib.2017.11.013.

Schäfer W, Eckart RA, Schmid B, Cagköylü H, Hof K, Muller YA, et al. Nuclear trafficking of the anti-apoptotic *Coxiella burnetii* effector protein AnkG requires binding to p32 and importin-α1. Cell Microbiol. 2017;19: e12634. https://doi.org/10.1111/cmi.12634.

Shanmugam SK, Dalbey RE. The conserved role of YidC in membrane protein biogenesis. Microbiol Spectr. 2019;7:7.1.02. https://doi.org/10.1128/microbiolspec.PSIB-0014-2018.

Stewart M. Molecular mechanism of the nuclear protein import cycle. Nat Rev Mol Cell Biol. 2007;8:195–208. https://doi.org/10.1038/nrm2114.

Szurek B, Marois E, Bonas U, Van den Ackerveken G. Eukaryotic features of the *Xanthomonas* type III effector AvrBs3: protein domains involved in transcriptional activation and the interaction with nuclear import receptors from pepper. Plant J. 2001;26:523–34. https://doi.org/10.1046/j.0960-7412.2001.01046.x.

Wagner S, Grin I, Malmsheimer S, Singh N, Torres-Vargas CE, Westerhausen S. Bacterial type III secretion systems: a complex device for the delivery of bacterial effector proteins into eukaryotic host cells. FEMS Microbiol Lett. 2018;365:fny201. https://doi.org/10.1093/femsle/fny201.

Wang J, Tian D, Gu K, Yang X, Wang L, Zeng X, et al. Induction of *Xa10*-like genes in rice cultivar Nipponbare confers disease resistance to rice bacterial blight. Mol Plant Microbe Interact. 2017;30:466–77. https://doi.org/10.1094/MPMI-11-16-0229-R.

Wang X, Zhang L, Ji H, Mo X, Li P, Wang J, et al. Hpa1 is a type III translocator in *Xanthomonas oryzae* pv. *oryzae*. BMC Microbiol. 2018;18:105. https://doi.org/10.1186/s12866-018-1251-3.

White FF, Potnis N, Jones JB, Koebnik R. The type III effectors of *Xanthomonas*. Mol Plant Pathol. 2009;10:749–66. https://doi.org/10.1111/j.1364-3703.2009.00590.x.

Wirthmueller L, Roth C, Banfield MJ, Wiermer M. Hop-on hop-off: importin-α-guided tours to the nucleus in innate immune signaling. Front Plant Sci. 2013;4:149. https://doi.org/10.3389/fpls.2013.00149.

Wirthmueller L, Roth C, Fabro G, Caillaud MC, Rallapalli G, Asai S, et al. Probing formation of cargo/importin-α transport complexes in plant cells using a pathogen effector. Plant J. 2015;81:40–52. https://doi.org/10.1111/tpj.12691.

Xiong F, Groot EP, Zhang Y, Li S. Functions of plant importin β proteins beyond nucleocytoplasmic transport. J Exp Bot. 2021;72:6140–9. https://doi.org/10.1093/jxb/erab263.

Yang B, Sugio A, White FF. *Os8N3* is a host disease-susceptibility gene for bacterial blight of rice. Proc Natl Acad Sci USA. 2006;103:10503–8. https://doi.org/10.1073/pnas.0604088103.

Yang C, Yu Y, Huang J, Meng F, Pang J, Zhao Q, et al. Binding of the *Magnaporthe oryzae* chitinase MoChia1 by a rice tetratricopeptide repeat protein allows free chitin to trigger immune responses. Plant Cell. 2019;31:172–88. https://doi.org/10.1105/tpc.18.00382.

Yoo SD, Cho YH, Sheen J. *Arabidopsis* mesophyll protoplasts: a versatile cell system for transient gene expression analysis. Nat Protoc. 2007;2:1565–72. https://doi.org/10.1038/nprot.2007.199.

Yuan M, Ke Y, Huang R, Ma L, Yang Z, Chu Z, et al. A host basal transcription factor is a key component for infection of rice by TALE-carrying bacteria. Elife. 2016;5: e19605. https://doi.org/10.7554/eLife.19605.

Zhai Y, Li P, Mei Y, Chen M, Chen X, Xu H, et al. Three *MYB* genes co-regulate the phloem-based defence against English grain aphid in wheat. J Exp Bot. 2017;68:4153–69. https://doi.org/10.1093/jxb/erx204.

Zhang Y, Su J, Duan S, Ao Y, Dai J, Liu J, et al. A highly efficient rice green tissue protoplast system for transient gene expression and studying light/chloroplast-related processes. Plant Methods. 2011;7:30. https://doi.org/10.1186/1746-4811-7-30.

Zhang L, Chen L, Dong H. Plant aquaporins in infection by and immunity against pathogens—a critical review. Front Plant Sci. 2019a;10:632. https://doi.org/10.3389/fpls.2019.00632.

Zhang L, Hu Y, Li P, Wang X, Dong H. Silencing of an aquaporin gene diminishes bacterial blight disease in rice. Australas Plant Pathol. 2019b;48:143–58. https://doi.org/10.1007/s13313-018-0609-1.

Zhao H, Zhang Y, Wu P, Wang J, Li H. The *Shigella* type three secretion system effector OspF invades host nucleus by binding host importin α1. World J Microbiol Biotechnol. 2019;35:71. https://doi.org/10.1007/s11274-019-2635-8.

Zhou Z, Bi G, Zhou JM. Luciferase complementation assay for protein-protein interactions in plants. Curr Protoc Plant Biol. 2018;3:42–50. https://doi.org/10.1002/cppb.20066.

Zipfel C, Robatzek S, Navarro L, Oakeley EJ, Jones JD, Felix G, et al. Bacterial disease resistance in *Arabidopsis* through flagellin perception. Nature. 2004;428:764–7. https://doi.org/10.1038/nature02485.